Environmental Science and Pollution Research (2018) 25:35276–35286
https://doi.org/10.1007/s11356-018-3439-3

RESEARCH ARTICLE

# Novel ceramic paper structures for diesel exhaust purification

Sabrina A. Leonardi[1] · Fernando E. Tuler[1] · Eric M. Gaigneaux[2] · Damien P. Debecker[2] · Eduardo E. Miró[1] · Viviana G. Milt[1]

Received: 13 April 2018 / Accepted: 10 October 2018 / Published online: 19 October 2018


## Abstract

The catalytic combustion of diesel soot is addressed with flexible and structured "paper catalysts". Two different series of catalysts were prepared either by drip impregnation or by a spray method to deposit a mixture of Co, Ba, and K or a mixture of Co and Ce onto $SiO_2$-$Al_2O_3$ ceramic paper matrixes. In every case, $CeO_2$ nanoparticles were added to bind the ceramic fibers. SEM images showed that the impregnation method generated catalytic particles concentrated as large chunks (> 10 μm), mainly at ceramic fiber crossings, whereas the spray method produced smaller catalytic particles (< 1 μm) well distributed throughout the ceramic paper. Besides, Co-Ba-K particles appeared better dispersed on the surface of ceramic fibers than Co-Ce due to the presence of K. Additionally, FTIR spectra showed the formation of $O_2^{2-}$ and $O_2^-$ species associated with $CeO_2$ (binder) on the samples containing potassium which gave the Co-Ba-K-ceramic paper good catalytic properties, thus making the Co-Ba-K drop impregnated the best catalyst both considering activity and stability. Successive temperature programmed oxidation (TPO) runs up to 700 °C caused the formation of cobalt silicates in the catalytic ceramic paper prepared by the spray method, as indicated by TPR. The formation of these species was probably favored by the smaller size of cobalt particulates and their higher dispersion in the catalysts prepared by the spray method. This provoked the partial loss of the redox properties of $Co_3O_4$. TPR experiments also indicated the formation of $BaCoO_3$ in Ba-containing ceramic paper, which could help in maintaining the catalyst activity after several TPO runs through the capacity of this mixed perovskite-type oxide to trap and release $NO_x$.

**Keywords** Cobalt, barium, potassium · Cerium · Catalytic ceramic paper · Structured catalysts · Diesel soot combustion · Spray deposition

## Introduction

During the last decade, fiber materials have gained in popularity for catalytic applications due to the benefits associated with the high surface to volume ratio and the high void fractions offered by these structures. Based on the preparation method the fibrous substrates can be fitted to various geometries. Also, they exhibit lower costs and a better coatability compared to microchannel reactors. The variety of different fiber based catalyst supports is large and each type of support shows its own advantages, as a function of the chosen fiber material and manufacturing process (Reichelt et al. 2014). An interesting possibility is to shape the fibers as papers that can be easily rolled-up inside cartridges that, for example, can be useful to develop catalytic filters for the abatement of diesel soot particles. The development of new and more efficient processes for the abatement of diesel contaminants has renewed its public concern since the classification by the World Health Organization of the soot particles as carcinogenic grade 1 and also since the recent Volkswagen scandal.

Nowadays, commercialized filters consist of SiC monoliths with active elements on it (Quiles-Díaz et al. 2015; Aneggi et al. 2014; Liu et al. 2015; Tuler et al. 2015a). As an alternative, our group proposed to use the

Responsible editor: Philippe Garrigues

**Electronic supplementary material** The online version of this article (https://doi.org/10.1007/s11356-018-3439-3) contains supplementary material, which is available to authorized users.

✉ Damien P. Debecker
damien.debecker@uclouvain.be

✉ Viviana G. Milt
vmilt@fiq.unl.edu.ar

[1] Instituto de Investigaciones en Catálisis y Petroquímica, INCAPE, CONICET, Facultad de Ingeniería Química, Universidad Nacional del Litoral, Santiago del Estero 2829, 3000 Santa Fe, Argentina

[2] Institute of Condensed Matter and Nanosciences (IMCN), UCLouvain, Place Louis Pasteur 1 box L4.01.09, 1348 Louvain-La-Neuve, Belgium

mentioned ceramic papers as suitable materials to conform flexible structured catalysts and diesel filters (Tuler et al. 2014; Koga et al. 2006, 2008a, b, 2009; Ishihara et al. 2010). Ceramic papers present suitable mechanical properties to resist assays from a test bench in which they were placed inside a metal housing, at the exhaust pipe outlet of a Corsa 1.7 diesel vehicle (Tuler et al. 2014). Optimal mechanical properties were obtained through the incorporation of a suspension of $CeO_2$ nanoparticles as a binder (10 or 20 wt.% $CeO_2$) during the papermaking process. The passive regeneration of the filter however requires the addition of catalytic components (Piumetti et al. 2016).

In this work, we present a systematic study performed with the aim of preparing active and stable catalytic filters for the abatement of diesel soot particulates. These filters are prepared from $SiO_2$-$Al_2O_3$ ceramic fibers arranged under the form of papers discs using the papermaking process. These papers have been useful to trap soot particles from the exhausts of a real diesel engine (Tuler et al. 2014). In order to continuously regenerate the filters, a catalytic phase must be firmly attached to the ceramic fibers and, at the same time, the catalytic particles should be highly dispersed throughout the paper and small enough to be catalytically efficient to burn the soot under working conditions. To this end, in this work, we explore two methods for the incorporation of the catalytic particles: drip impregnation and spray deposition. The first method involves the impregnation by dripping a solution of precursor salts containing the desired catalytic components directly on the paper support, followed by calcination. The second one is inspired by the aerosol process (Tuler et al. 2015b; Debecker et al. 2018), which is currently emerging as a powerful tool for the preparation of advanced materials, especially catalysts (Colbeau-Justin et al. 2014; Debecker et al. 2012, 2014; Maksasithorn et al. 2015; Pega et al. 2009). We chose two active formulations that have already proved to be active in previous works but having different catalytic properties: Co-Ba-K and Co-Ce (Tuler et al. 2015a, b). The first formulation takes advantage of the redox capacity of cobalt oxide that is enhanced by the high availability of surface oxygen species of ceria. The second one also features the high oxidative potential of cobalt but additionally incorporates the capacity of Ba and K to form nitrate species which are known to be also active for soot oxidation (Zhang et al. 2018). Also, K is known to allow increasing the soot-to-catalyst interaction. The prepared structured catalysts were evaluated for soot combustion (temperature programmed oxidation TPO experiments) in terms of the activity characterized by the maximum combustion rate temperature, and stability during successive TPO runs. In order to correlate the catalytic measurements with physical chemistry properties, both fresh and used catalysts were characterized by TPR, XRD, SEM, and FTIR.

## Experimental

### Ceramic paper preparation

Following a procedure previously in detail described (Tuler et al. 2014) ceramic paper discs (16.5 cm in diameter) were prepared from ceramic fibers ($SiO_2$-$Al_2O_3$), which were dispersed in an aqueous medium where also a binder was added (20 wt.% of $CeO_2$ nanoparticles, Nyacol). Cellulose fibers were also incorporated to enhance the retention of the ceramic fibers during the mat formation, along with cationic and anionic polymers: polyvinylamine (PVAm) and anionic polyacrylamide (A-PAM), respectively.

A two-step method was employed for the preparation of catalytic ceramic papers. In the first step, following the papermaking technique, a sheet was formed and dried under controlled atmosphere (23 °C, 50% R.H.) for 24 h and finally calcined in air at 600 °C for 2 h. The second step corresponded to the deposition of the catalytic ingredients. Two series of catalysts were prepared, one adding Co, Ba, and K and the other incorporating Co and Ce from their corresponding nitrate solutions as will be explained below. It must be pointed out that Ce oxide (Nyacol) was also incorporated as a binder in both formulations, which mainly accumulates as patches of about 5 μm in the fiber crossings due to capillary forces exerted during the drying step. Thus, both formulations (Co-Ba-K and Co-Ce) contain $CeO_2$ as the binder. Two methods were used to incorporate the catalytic components: the conventional dripping method and the spray technique.

### Drip impregnation

#### Co-Ce-catalytic ceramic paper

The incorporation of the catalytic ingredients by drip impregnation was carried out using a solution of $Ce(NO_3)_3$ and $Co(NO_3)_2$, which was prepared by dissolving the necessary amount of each precursor salt in the volume of water calculated to saturate the paper structure, so as to load 4 wt.% of $Ce(NO_3)_3 + Co(NO_3)_2$ (weight ratio Ce:Co = 2.37:1). The impregnated ceramic paper discs were then dried at room temperature overnight and calcined in a furnace at 600 °C for 2 h. The catalysts were denoted as Co-Ce-I.

#### Co-Ba-K-catalytic ceramic paper

The incorporation of the catalytic ingredients by drip impregnation was carried out using a solution of $Ba(CH_3COO)_2$, $KNO_3$ and $Co(NO_3)_2$ (weight ratio Ba:K:Co = 1.33:0.58:1), which was prepared by dissolving the necessary amount of each precursor salt in the volume of water calculated to

saturate the paper structure, so as to load 5 wt.% of catalyst (expressed as Co + Ba + K per gram of ceramic fiber). The impregnated ceramic paper discs were then dried at room temperature overnight and calcined in a furnace at 600 °C for 2 h. The catalysts were denoted as Co-Ba-K-I.

## Spray deposition

### Co-Ce-catalytic ceramic paper

In the second case, a mixed solution of $Ce(NO_3)_3$ (0.622 g/l) and $Co(NO_3)_2$ (0.556 g/l) was placed in an atomizer (6-Jet 9306A atomizer from TSI) and sprayed with an air pressure of 30 psi. The aerosol was partially dried by quickly passing through a tubular furnace heated at 400 °C (residence time of about 1 s) and then the particles were directly sprayed onto the ceramic papers. Any excess particles exiting across the paper were retained by an absolute filter. The spraying time (6–8 h) was adjusted in order to load 4 wt.% $Ce(NO_3)_3 + Co(NO_3)_2$ on the ceramic paper discs. The sprayed ceramic papers were then calcined in a furnace at 600 °C for 2 h. The actual loading was verified by weighing. Catalytic papers are denoted as Co-Ce-S.

### Co-Ba-K-catalytic ceramic paper

Similarly, as previously described, a mixed solution containing 0.056 g/ml $Ba(CH_3COO)_2$, 0.111 g/ml $Co(NO_3)_2$, and 0.034 g/ml $KNO_3$ was placed in the atomizer (6-Jet 9306A atomizer from TSI), the aerosol produced was passed through a tubular furnace set at 400 °C and the particles were sprayed onto the ceramic paper discs. After 6 h of spraying, 4.4 wt.% of active species were loaded on the ceramic paper pieces. Finally, the sprayed ceramic discs were calcined at 600 °C for 2 h. Thus obtained, catalytic papers were denoted as Co-Ba-K-S.

## Characterization

Crystalline phases were determined with a Shimadzu XD-D1 instrument with monochromator using CuKα radiation at a scan rate of 2°/min, from 2θ = 15° to 80°. The pieces of about 16 mm in diameter were supported in a special sample holder designed for the XRD analysis. The software package of the equipment was used for the phase identification from the X-ray diffractograms.

Microscopic images were obtained with a SEM Jeol JSM-35C equipment was employed operated at 20 kV acceleration voltage. Samples were glued to the sample holder with Ag painting and then coated with a thin layer of Au in order to improve the images.

Fourier Transform Infrared Spectroscopy (FTIR) was used to identify the functional groups. Samples were prepared in the form of pressed wafers (ca. 1% sample in KBr). A Shimadzu IR Prestige-21 spectrometer was utilized to obtain the infrared spectra. All spectra involved the accumulation of 40 scans at 8 $cm^{-1}$ resolution.

The elemental chemical analysis was performed by EDS using an energy dispersive instrument—Phenom model Word ProX (Netherlands)—operated at 15 kV of acceleration voltage, on several zones of the samples. Also, the mapping of bigger areas was carried out. Semi quantitative results were obtained with the theoretical quantitative method (SEMIQ), which does not require standards.

Temperature-programmed reduction (TPR) was used to study the reducibility of the catalysts. The experiments were run on a Micromeritics Autochem II instrument with a TCD detector. The reducing gas flow was 5% $H_2$ in Ar, heating the samples from room temperature to 1000 °C at a heating rate of 10 °C $min^{-1}$.

## Soot combustion experiments (temperature programmed oxidation)

Soot particles were produced by burning a commercial diesel fuel (YPF, Argentina) in a glass vessel. After being collected from the vessel walls, the soot was dried in a stove at 120 °C for 24 h. Soot particles were dispersed in n-hexane using an ultrasonic bath in order to obtain a homogeneous suspension of 600 ppm of diesel soot in n-hexane. The incorporation of soot particles to the ceramic paper pieces (1.6 cm in diameter discs) was carried out by adding the suspension dropwise until saturation, and then drying at room temperature.

The catalytic activity of the ceramic papers for the soot combustion was studied by temperature-programmed oxidation (TPO). For this purpose, the structured samples loaded with the soot were heated at 5 °C/min from room temperature up to 600 °C in $O_2$ (18%) + NO (0.1%) diluted in He (total flow 20 ml/min) in a flow equipment designed for this purpose. The exhaust gases were analyzed with a Shimadzu GC-2014 chromatograph (with TCD detector). In order to evaluate the stability of the systems, five successive cycles were performed, the first two up to 600 °C and the following three up to 700 °C. Between each cycle, the catalytic ceramic disc was removed from the set-up and soot was incorporated into the sample as previously described. Since the non-catalytic soot combustion occurs at about 550 °C, the final temperature of each TPO run ensured the complete removal of the loaded soot, so that the contact between the fresh soot and the catalyst is the same at the beginning of each TPO experiment and the differences in activity reflect the catalyst deactivation. After the five cycles, samples were characterized and named with an asterisk.

## Results and discussion

In a previous work (Tuler et al. 2015b) we prepared catalytic ceramic paper by the spray method adding two catalytic components, cobalt and cerium. We demonstrated the efficiency of this method to homogeneously disperse small catalytic particles on ceramic fibers. The structured catalysts thus obtained burnt soot with a maximum in the TPO profiles at about 400 °C. To further study this system, successive TPO runs were carried out to check catalytic stability. But also, and with the aim of enhancing catalytic activity, other components were added as catalytic ingredients: cobalt, barium and potassium, the last two aim at trapping $NO_x$ and favoring the soot-to-catalyst contact, respectively. A series of experiments was carried out in parallel adding the catalysts to the ceramic paper either by the spray method or using the more traditional impregnation one.

### Scanning electron microscopy and energy dispersive X-ray spectroscopy

SEM images (Fig. 1) show that ceramic paper is an open structure formed by a matrix of ceramic fiber, where catalytic particles appear distributed along the fibers. As previously seen (Tuler et al. 2015b), the sample prepared by the impregnation method containing cobalt and cerium, Co-Ce-I, exhibits catalytic particles concentrated as large chunks (> 10 μm) heterogeneously distributed along the fibers, and deposited in the fiber crossings where the binder is mainly accumulated. (Fig. 1a), whereas the spray method produced smaller catalytic particles (< 1 μm, Fig. 1b) well distributed throughout the ceramic paper (Co-Ce-S). No significant differences were observed in the case of Co-Ba-K-containing ceramic paper, compared to Co-Ce ones. The traditional impregnation method (Fig. 1c, e) produces larger particles than the spray one (Fig. 1d, f).

The catalytic component distribution was studied by EDS analysis (mapping). Figure 2 shows images obtained for impregnated and sprayed samples. Although as said before the distribution of particles is different in the catalytic papers obtained using both methods, in the case of Co-Ba-K samples (both Co-Ba-K-I and Co-Ba-K-S) catalytic components (Co, Ba, and K) appear well distributed all along the structure covering the ceramic fibers and forming catalytic agglomerates, which is not the case of both Co-Ce samples (Co-Ce-I and Co-Ce-S), where ceramic fibers appear to be mainly uncovered, and only the catalytic chunks are clearly observed. The better coverage in the samples containing K is most probably due from the formation of potassium salts and oxides of low melting point, favoring the distribution of catalytic components all along ceramic fibers.

### Infrared spectroscopy

Figure 3a shows infrared spectroscopy (FTIR) spectra of catalytic ceramic papers, where the spectrum of bare ceramic fibers is also included for comparison. This last exhibits a broad band at 1000–1200 $cm^{-1}$ due to Si-O stretching of $SiO_2$ ceramic fibers, which also appears in the spectra of the catalytic ceramic papers. Besides, all spectra exhibit the signal at 667 $cm^{-1}$, associated to Co-O stretching of $Co^{2+}$ in the $Co_3O_4$ spinel (Khalaji et al. 2014). No other defined signals could be ascribed in the IR spectra of Co-Ce-containing ceramic paper whereas for Ba,Co,K-containing samples, small signals at 1069, 1110 and 1180 $cm^{-1}$ appear. These peaks correspond to peroxide ($O_2^{2-}$) or superoxide ($O_2^{-}$) species associated to $CeO_2$ and preferentially formed in the presence of K. K indeed could be inserted into the $CeO_2$ lattice and generate anionic vacancies increasing the number of peroxide and superoxide species (Gross et al. 2012; Kaplin et al. 2017).

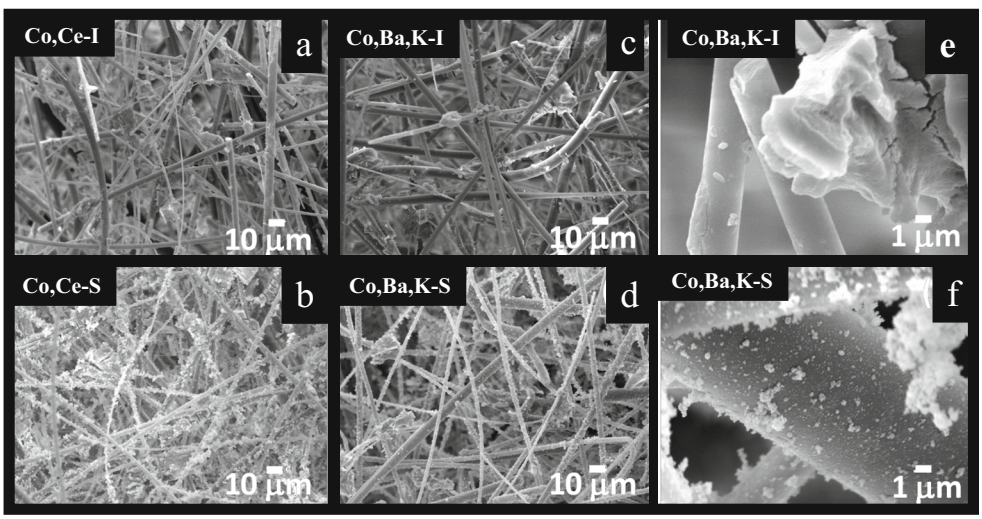


**Fig. 1** SEM micrographs of catalytic ceramic paper prepared either using the drip impregnation procedure (**a**, **c**, and **e**) or the spray method (**b**, **d**, and **f**)

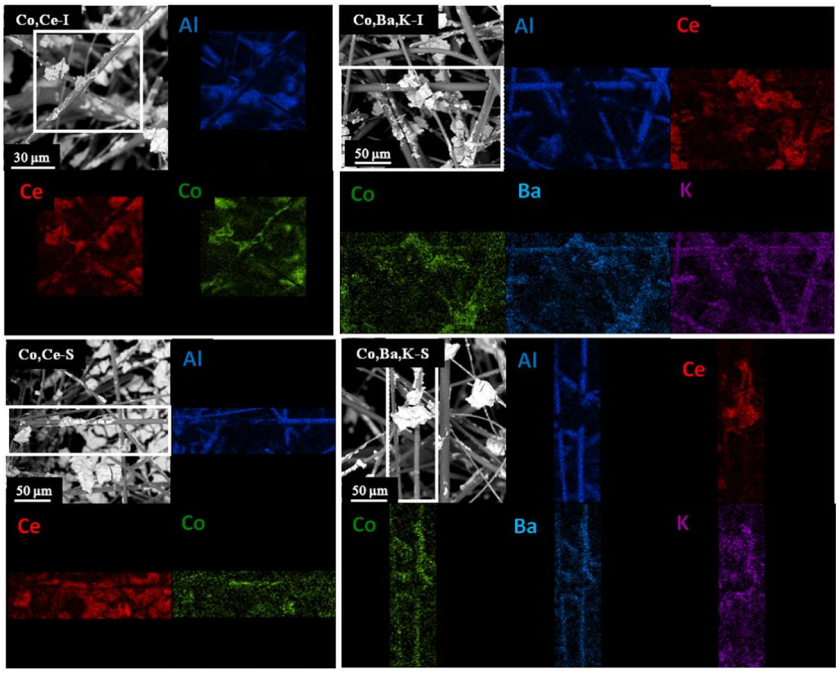


**Fig. 2** Distribution of catalytic components throughout ceramic paper prepared by drip impregnation or by the spray technique (EDS mapping)

## Temperature-programmed reduction

The reducibility of the catalytic ceramic papers was studied by TPR (Fig. 3b). Co-Ce-containing catalysts show different profiles according to the preparation protocol. The TPR profile corresponding to Co-Ce-I could be convoluted considering six peaks with different intensities (very strong, vs; medium, m; and weak, w), with maxima at 355 (vs), 400 (m), 442 (vs), 480 (m), 686 (w) and 758 °C (m) (Fig. 2S). The overlapped peaks at 355 and 442 °C correspond to $Co_3O_4$ reduction ($Co^{3+} \rightarrow Co^{2+}$ and $Co^{2+} \rightarrow Co°$, respectively); the peak with a maximum at 400 °C corresponds to $CeO_2$ (surface) reduction,

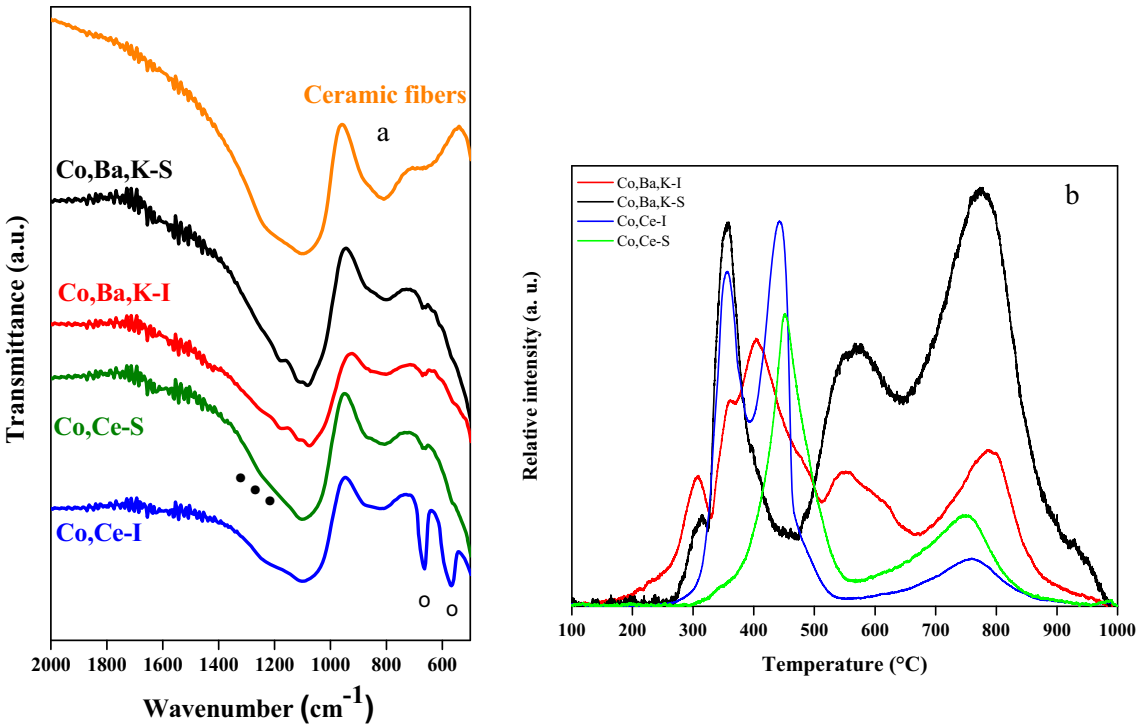


**Fig. 3** (**a**) Infrared spectra of catalytic systems (o $Co_3O_4$ and • peroxide and superoxide species) and (**b**) TPR profiles

which is reported to occur between 290 and 465 °C (Jin et al. 2016; Gómez et al. 2016), whereas the peak at 480 °C (tailoring) could be associated to a wide distribution of sizes of cobalt particles. The signal with maximum at 686 °C could be ascribed to the $CoAl_2O_4$ spinel reduction to Co° and the peak at 758 °C could be associated with bulk $CeO_2$ reduction (Liotta et al. 2006; Han et al. 2015). In the case of Co-Ce-S, the corresponding TPR profile is similar to that of Co-Ce-I and it was fitted considering five reduction peaks, with maxima at 359 (w), 445 (vs), 483 (m), 688 (m), and 758 °C (m) (Fig. 2S). The main difference between the impregnated and the sprayed samples appears in the 320–480 °C region, associated with $Co_3O_4$ reduction. According to Tarka et al. (2017) (Potoczna-Petru and Kepinski 2001), smaller $Co_3O_4$ particles are harder to reduce and the spray method favors the formation of smaller particles (SEM images, Fig. 1). Besides, $CeO_2$ promotes $Co_3O_4$ dispersion, favoring the formation of smaller crystallites. This explains why the sprayed sample exhibits lower intensity peaks in the 320–480 °C zone and a bigger one at 483 °C (Luo et al. 2008).

TPR profiles of Co-Ba-K-containing catalysts are more complex (Fig. 3) and the corresponding fittings are shown in (Fig. 3S). In the case of Co-Ba-K-I, the peaks at 305 (m) and 354 °C (s) correspond to $Co_3O_4$ reduction that occurs at lower temperatures if compared to Co-Ce-containing catalysts probably due to the higher accessibility of $H_2$ to cobalt particles originated by the presence of K, which enhanced catalyst dispersion (as seen by EDS). At 404 °C, a very strong signal is observed, which, according to previous works (Milt et al. 2005; Xu et al. 2016), could correspond to $BaCoO_{3-y}$ perovskite-type oxide reduction. The shoulder at 473 °C (m) could correspond, as previously described, to cobalt reduction at the interface $Co_3O_4$ - $CeO_2$ ($Co^{2+} \rightarrow Co°$), associated to the presence of different sizes of cobalt particles. The two overlapped signals with maxima at about 545 (s) and 614 °C (m) could be associated to $KNO_3$ reduction (Mosconi et al. 2007), whereas at higher temperatures (ca. 780 °C), the wide and intense peak could involve $CoAl_2O_4$ along with bulk $CeO_2$ reduction. If compared with Co-Ce-catalysts, this high-temperature peak is considerably higher in the Ba-containing samples and appears at slightly higher temperatures. A similar effect was observed by Marrero-Jerez et al. (Marrero-Jerez et al. 2014) when studying gadolinia-doped $CeO_2$ supported on $Al_2O_3$: the increase in Gd content resulted in a shift towards higher temperatures of the peak associated to bulk $Ce^{+4}$ reduction and also, in an increment in the area beneath the TPR peak. Also, the reduction of the $BaCeO_3$ perovskite should be considered (Yang et al. 2010).

In the case of the sprayed sample (Co-Ba-K-S), the TPR profile is similar to that of Co-Ba-K-I, the main differences being the much less intense peak at 402 °C and the absence of the peak at 475 °C, as previously discussed, associated with the presence of the $BaCoO_{3-y}$ perovskite-type oxide and with the different sizes of cobalt particles, respectively. Probably, the traditional impregnation method favors the $BaCoO_{3-y}$ perovskite formation whereas in the spray method, the partial drying of aerosol droplets when they pass through the furnace at 400 °C produces more homogeneous sizes of particles. Besides, as previously described, smaller $Co_3O_4$ particles are more difficult to reduce. On the other hand, the bigger peak at 780 °C should correspond to $BaCO_3$ reduction, present in higher amounts in the sprayed sample (Co-Ba-K-S), along with $BaCeO_3$ reduction.

## X-ray diffraction

Figure 4 shows XRD patterns. Both Co-Ce-S and Co-Ce-I show signals corresponding to the $CeO_2$ fluorite-type oxide (JCPDS # 34–394). No signals associated with cobalt species appear, indicating their high dispersion (small particle size). However, if considering the cobalt percentage in the catalyst (12 wt.%) and the amount of catalyst loaded on the ceramic paper (5 wt.%), it is probably that the cobalt content is close to the detection limit of the technique. In the case of Co-Ba-K-containing ceramic papers, the XRD pattern of the impregnated sample (Co-Ba-K-I) shows, besides $CeO_2$ signals, others associated to $BaCO_3$ (JCPDS # 45–1471). The sprayed sample (Co-Ba-K-S) also show the $BaCO_3$ signals, but with a much lower intensity, accounting for a higher dispersion of $BaCO_3$ particles (Fig. 1).

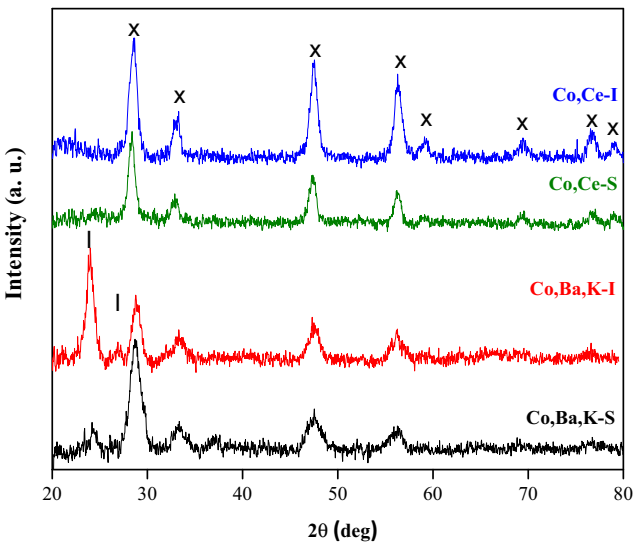


**Fig. 4** XRD diffraction patterns of catalytic ceramic. Symbols: I $BaCO_3$ and x $CeO_2$

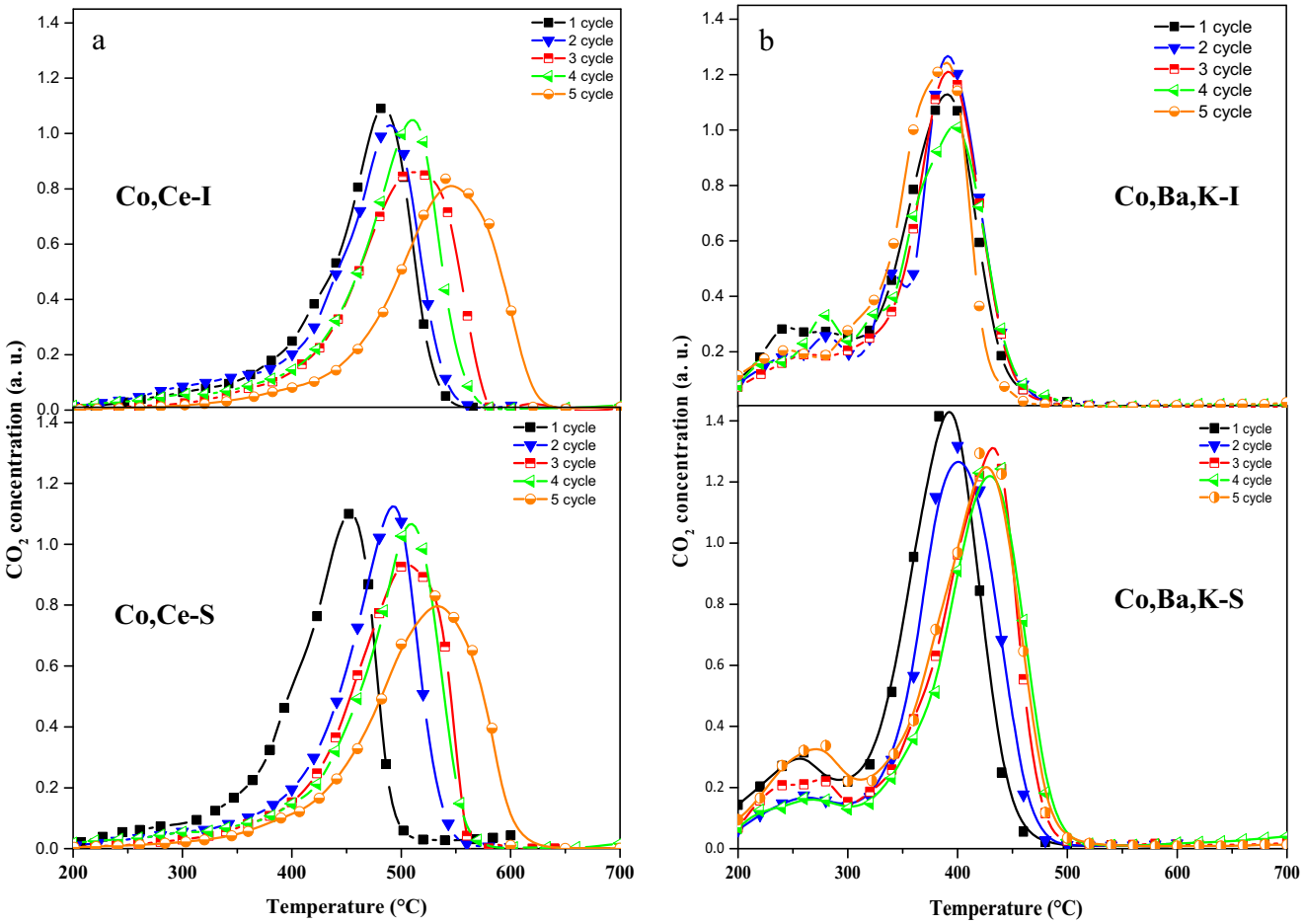


**Fig. 5** TPO stability runs of catalytic ceramic paper containing (**a**) Co-Ce and (**b**) Co-Ba-K

## Catalytic evaluation (TPO)—stability runs

In a previous work (Tuler et al. 2015b), we observed that the incorporation of cobalt and cerium by the spray technique (Co-Ce-S catalyst) resulted in a more active catalyst than that prepared by the traditional impregnation technique (Co-Ce-I catalyst). However, stability is as important as activity, and unfortunately, the structured catalysts prepared by the spray technique did not behave well in cycling experiments. Thus, in this work, the stability of the drip impregnation and spray-made catalysts was further studied.

The two first TPO runs for Co-Ce-I up to 600 °C indicated that no deactivation was observed (Fig. 5a). Nevertheless, after the three successive TPO runs up to 700 °C, a partial deactivation of the catalysts occurred, as observed by the shift in the TPO profiles to higher temperatures. The temperature of maximum reaction rate indicated that after the five TPO runs, $T_M$ values shifted from 480 °C to 540 °C (Table 1). The sprayed sample (Co-Ce-S) was initially more active with a $T_M$ value of 453 °C for the first run and started to deactivate already after the first TPO run (Fig. 5a). Then, $T_M$ values progressively shift down to 530 °C for the fifth run, i.e., still slightly better than Co-Ce-I (Fig. 5a and Table 1).

Co-Ba-K-containing ceramic papers were more active and stable if compared with those containing cobalt and cerium. For Co-Ba-K-S, the temperature of maximum combustion rate of the first run was as low as 390 °C and after a slight deactivation in the first two cycles, the $T_M$ was maintained around 428 °C in the next three cycles (Fig. 5b and Table 1). However, the impregnated ceramic paper (Co-Ba-K-I) performed even better, both considering activity and stability. In fact, a $T_M$ of 390 °C was maintained from the first to the fifth TPO run.

As Fig. 6 summarizes, there is a marked difference in the catalytic activity of the systems containing either Co-Ce or

**Table 1** Temperature (°C) of maximum combustion rate of soot

| Catalytic ceramic paper | TPO cycles | | | | |
|---|---|---|---|---|---|
| | 1 | 2 | 3 | 4 | 5 |
| Co,Ba,K-S | 390 | 400 | 430 | 428 | 428 |
| Co,Ba,K-I | 390 | 390 | 390 | 400 | 390 |
| Ce,Co-S | 453 | 492 | 504 | 508 | 530 |
| Ce,Co-I | 480 | 488 | 508 | 508 | 540 |

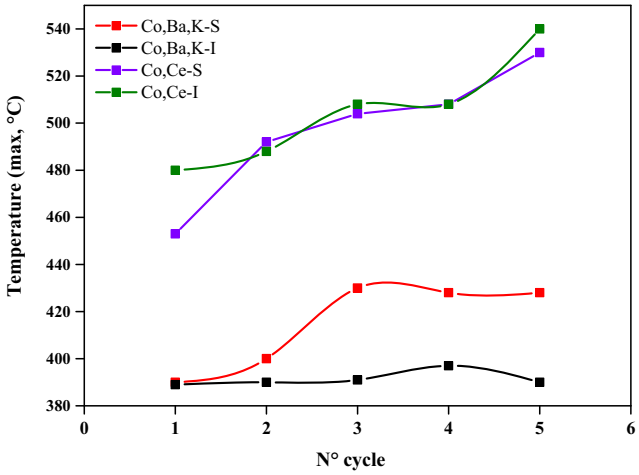


**Fig. 6** Variation of the temperature of maximum combustion rate during successive TPO runs (values extracted from Fig. 5)

Co-Ba-K, the latter being more active. For these catalysts, it is important to note the beneficial effect of NO in the gas phase, which catalyzes soot combustion from the NO – $NO_2$ redox cycle, and the presence of $KNO_3$, which favors soot to catalyst contact owing to its low fusion temperature and also provides additional active sites (Gross et al. 2009). Besides, peroxide and superoxide species (detected by FTIR), preferentially formed in the presence of potassium, enhance soot burning abilities of Co-Ba-K-the catalysts. Remarkably, the Co-Ba-K-I catalytic ceramic paper showed a very good activity and stability. In fact, the $T_M$ value is close to the temperature of diesel exhaust gases, which potentiates the applicability of this system.

## Catalyst characterization after stability runs

SEM images of catalytic ceramic papers after stability runs (Fig. 7) show no significant differences if compared with images of fresh samples (Fig. 1): big catalytic aggregates (> 10 μm) are present on impregnated samples (Co-Ce-I* and Co-Ba-K-I*), whereas for sprayed samples, smaller aggregates of catalyst (< 1 μm) are observed after the successive TPO runs (Co-Ce-S* and Co-Ba-K-S*). Besides, EDS mapping (Fig. 2S, Supplementary Information) shows no changes in the catalytic species distribution before and after the stability run, which implies the good anchoring of catalytic species deposited from both methods. It is worth mentioning that catalytic particles are incorporated partially dried when applying the spray method ensuring particle anchoring.

In order to elucidate why do some catalytic ceramic papers deactivate and why Co-Ba-K-I did maintain its good performance, FTIR and TPR techniques were used. FTIR spectra shown in Fig. 8a show that all catalysts exhibit the bands at 667 and 565 $cm^{-1}$ associated with the Co-O bond stretching of $Co_3O_4$, appearing better defined for Co-Ba-K-I*, and although these signals were better observed for Co-Ce-I (Fig. 3a), their intensities decreased after the stability runs. This is probably linked to the catalytic stability of Co-Ba-K-I.

Additionally, TPR studies help understanding this behavior (Fig. 8b and the corresponding convolutions in the Supplementary Information Section). Figure 2S compares TPR profiles of catalysts impregnated with cobalt and cerium before and after the stability runs (i.e., Co-Ce-I and Co-Ce-I*). The main difference between both TPR profiles is the almost complete disappearance of the lowest temperature reduction peak, associated to $Co^{3+} \rightarrow Co^{2+}$ in $Co_3O_4$, in agreement with FTIR. Also, the wide peak at higher temperatures increases for the evaluated sample. This peak was convoluted considering two peaks with maxima at 680 and 750 °C respectively, the first one corresponding to the reduction of $Co^{2+}$ in $CoAl_2O_4$ spinel into $Co^0$ and the last one, to the reduction of bulk $CeO_2$. The formation of the $CoAl_2O_4$ spinel from $Co_3O_4$ appears as the main cause of Co-Ce-I deactivation.

In the case of the sprayed sample, the TPR profiles of Co-Ce-S and Co-Ce-S* are similar, although some differences appear at high temperatures: the maximum of the wide peak is shifted from 758 to 780 °C and it can be convoluted from three contributions with maxima at 690, 780 and 890 °C. The signal with maximum at 690 °C, as previously discussed, could be associated to the $CoAl_2O_4$ spinel reduction and the peak at 780 °C, to bulk $CeO_2$ reduction. The shift from 758 to 780 °C could be related to a stronger interaction between Ce and Al, favored from the excursions up to 700 °C during the stability runs, probably causing the formation of a binary Ce-Al mixed oxide. The peak with maximum at 890 °C could be assigned to cobalt silicate, formed due to small particles of cobalt strongly interacting with silica fibers (Ernst et al. 1999; Santos et al. 2012).

On the other hand, the TPR profile of Co-Ba-K-I* shows no significant differences before and after stability runs. Reduction peaks associated to $Co_3O_4$ and $BaCoO_{3-y}$ appear at temperatures below 410 °C, although the peak corresponding to $Co^{2+} \rightarrow Co^0$ appears completely overlapped to that corresponding to the perovskite $BaCoO_{3-y}$ reduction. The shoulder observed at 473 °C associated to the reduction of cobalt particles of different sizes appears as a separated peak after the catalytic evaluation whereas the peak caused by the reaction of $BaCoO_{3-y}$ appears a bit less intense. Probably, the ability of $BaCoO_{3-y}$ to reversibly trap and release $NO_x$ (Milt et al. 2005) helps maintaining the catalyst activity. Besides, it can be noticed that the only catalyst that shows a very low-temperature reduction peak, close to 250 °C, both before and after stability tests, is Co-Ba-K-I, which does not deactivate after stability runs. It is also important to remark that the wide peak, convoluted from two ones with maxima at 545 and 614 °C, is observed almost without any difference both before and after activity runs, which discards the occurrence of a

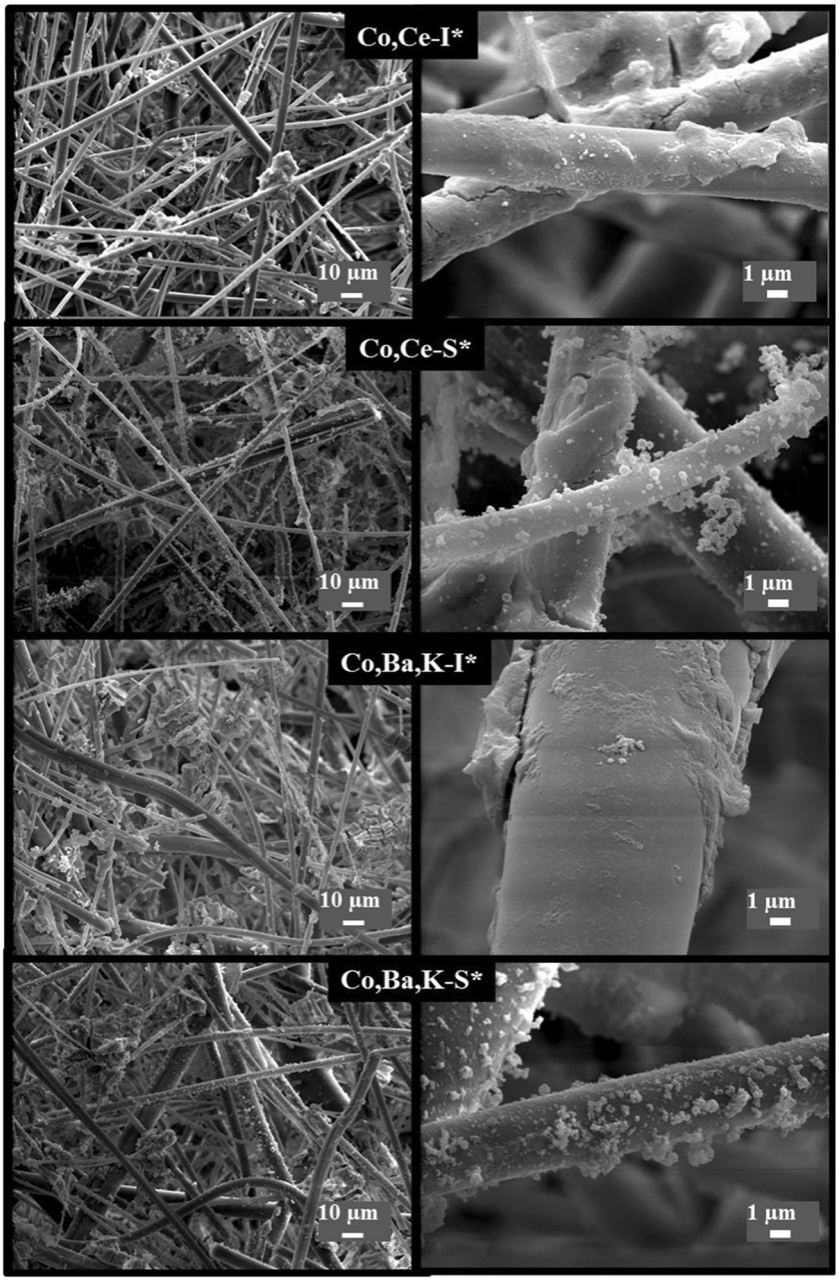


**Fig. 7** SEM micrographs of samples after stability runs (* samples): Co-Ce-I*, Co-Ce-S*, Co-Ba-K-I*, Co-Ba-K-S*

potassium loss. These results agree with the fact that maximum combustion rate temperatures keep almost constant (ca. 390 °C, Fig. 6).

The TPR profile of Co-Ba-K-S* is similar to that of the impregnated catalyst (Co-Ba-K-S), although the relative intensity of species more difficult to reduce vary. Besides, the high-temperature reduction peak at ca. 900 °C could be related to cobalt silicate formation, which may cause the catalyst deactivation after the third reaction cycle (Figs. 5 and 6). The better distribution of cobalt particles obtained by spray would favor cobalt silicate formation, since its corresponding reduction peak appears after stability runs of both samples prepared by the spray method.

Another important point to analyze is the effect of potassium addition. As seen in TPO experiments, different profiles are obtained for the samples containing K as compared with those without the alkaline metal, suggesting that different reaction processes occur. It is known that K favors the soot-to-catalyst contact, thus increasing the catalytic efficiency. However, the Co-Ba-K sprayed sample shows less stability than the impregnated one after five reaction cycles. This fact could be due to the presence of the $BaCoO_3$ phase in the impregnated sample, which may help in avoiding K loss at high temperatures, thus preserving catalytic activity. As discussed in our previous work (Milt et al. 2005) the incorporation of K into the perovskite lattice is possible due to the

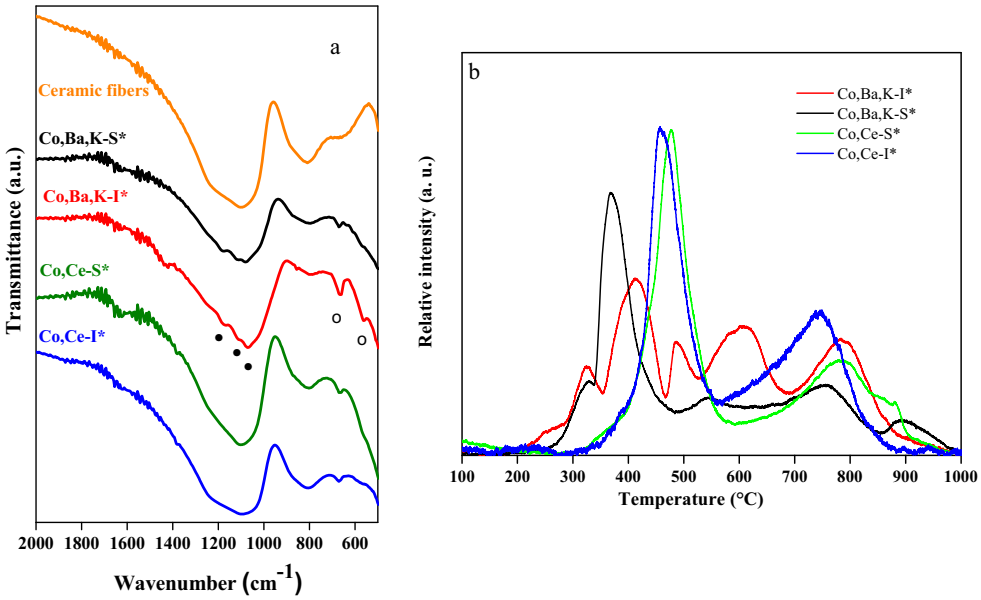


**Fig. 8** Characterization of catalytic systems after stability runs (* samples). (**a**) Infrared spectra (FTIR), o $Co_3O_4$ and • peroxide and superoxide species and (**b**) TPR profiles

similar ionic radii of Ba and K. In this vein, TPR profiles show no differences in intensity for the K reduction peak (545 °C – 615 °C) for Co-Ba-K-I and Co-Ba-K-I*. However, in the sprayed sample, although K is detected by EDS, TPR profiles indicate a loss of the alkaline metal (Fig. 3S).

## Conclusions

Co-Ba-K and Co-Ce catalysts deposited on ceramic paper either by drip impregnation or by the spray method were prepared and tested for soot combustion. Co-Ba-K resulted more active than Co-Ce for both preparation methods and Co-Ba-K drip impregnated was the best catalyst both in terms of activity and stability.

While Co-Ba-K particulates appeared well dispersed on the surface of ceramic fibers, this was not the case for Co-Ce. We attribute this to the presence of K in the former, probably responsible for the formation of mobile species during calcination. Besides, FTIR characterization showed the formation of peroxide and superoxide species associated to $CeO_2$ and preferentially formed in the samples containing potassium, most probably due to the formation of oxygen vacancies into the ceria lattice.

Successive runs up to 700 °C caused the formation of cobalt silicates in the catalytic ceramic papers prepared by the spray method, whose formation is favored for the smaller size of cobalt particulates and their higher dispersion specifically obtained via this preparation method. Consequently, the redox properties of $Co_3O_4$ are partially lost when these silicates form.

TPR experiments indicated the formation of $BaCoO_3$, which has a reduction peak at 400 °C, in Ba-containing ceramic papers. The capacity of this mixed perovskite-type oxide to trap and release $NO_x$ could help in maintaining the catalyst activity after several TPO runs. Indeed, the $T_M$ value is close to the temperature of diesel exhaust gases, which potentiates the applicability of this system.

**Funding information** This study received financial support from ANPCyT, CONICET, SECTEI Santa Fe and UNL (Argentina) and Program for Scientific and Technological Cooperation between the Ministry of Science, Technology and Productive Innovation of Argentina (MINCyT), and the Fonds de la Recherche Scientifique (FNRS) of the French Community of Belgium, BE/12/02.

## References

Aneggi E, Wiater D, de Leitenburg C, Llorca J, Trovarelli A (2014) Shape-dependent activity of ceria in soot combustion. ACS Catal 4:172–181

Colbeau-Justin F, Boissière C, Chaumonnot A, Bonduelle A, Sanchez C (2014) Aerosol route to highly efficient (Co) Mo/$SiO_2$ mesoporous catalysts. Adv Funct Mater 24:233–239

Debecker DP, Stoyanova M, Colbeau-Justin F, Rodemerck U, Boissière C, Gaigneaux EM, Sanchez C (2012) One-pot aerosol route to $MoO_3$-$SiO_2$-$Al_2O_3$ catalysts with ordered super microporosity and high olefin metathesis activity. Angew Chem Int Ed 15:2129–2131

Debecker DP, Stoyanova M, Rodemerck U, Colbeau-Justin F, Boissère C, Chaumonnot A, Bonduelle A, Sanchez C (2014) Aerosol route to nanostructured $WO_3$-$SiO_2$-$Al_2O_3$ metathesis catalysts: toward higher propene yield. Appl Catal A Gen 470:458–466

Debecker DP, Le Bras S, Boissiere C, Chaumonnot A, Sanchez C (2018) Aerosol processing: a wind of innovation in the field of advanced heterogeneous catalysts. Chem Soc Rev 47:4112–4155

Ernst B, Libs S, Chaumette P, Kiennemann A (1999) Preparation and characterization of Fischer–Tropsch active Co/$SiO_2$ catalysts. Appl Catal A Gen 186:145–168

Gómez LE, Múnera JF, Sollier BM, Miró EE, Boix AV (2016) Raman in situ characterization of the species present in Co/$CeO_2$ and Co/$ZrO_2$ catalysts during the COPrOx reaction. Int J Hydrog Energy 41: 4993–5002

Gross MS, Ulla MA, Querini CA (2009) Catalytic oxidation of diesel soot: new characterization and kinetic evidence related to the reaction mechanism on K/$CeO_2$ catalyst. Appl Catal A Gen 360:81–88

Gross MS, Ulla MA, Querini CA (2012) Diesel particulate matter combustion with $CeO_2$ as catalyst. Part I: system characterization and reaction mechanism. J Mol Catal A Chem 352:86–94

Han J-K, Jia L-T, Hou B, Li D-B, Liu Y, Liu Y-C (2015) Catalytic properties of $CoAl_2O_4/Al_2O_3$ supported cobalt catalysts for Fischer-Tropsch synthesis. J Fuel Chem Technol 43(7):846–851

Ishihara H, Koga H, Kitaoka T, Wariishi H, Tomoda A, Suzuki R (2010) Structured catalyst for catalytic NOx removal from combustion exhaust gas. Chem Eng Sci 65:208–213

Jin Q, Shen Y, Zhu S, Liu Q, Li X, Yan W (2016) Effect of praseodymium additive on $CeO_2(ZrO_2)/TiO_2$ for selective catalytic reduction of NO by $NH_3$. J Rare Earths 34(11):1111–1120

Kaplin IY, Lokteva ES, Golubina EV, Maslakov KI, Chernyak SA, Lunin VV (2017) Promoting effect of potassium and calcium additives to cerium–zirconium oxide catalysts for the complete oxidation of carbon monoxide. Kinet Catal 58:585–592

Khalaji AD, Nikookar M, Fejfarova K, Dusek M (2014) Synthesis of new cobalt(III) Schiff base complex: a new precursor for preparation $Co_3O_4$ nanoparticles via solid-state thermal decomposition. J Mol Struct 1071:6–10

Koga H, Fukahori S, Kitaoka T, Tomoda A, Suzuki R, Wariishi H (2006) Autothermal reforming of methanol using paper-like Cu/ZnO catalyst composites prepared by a papermaking technique. Appl Catal A Gen 309:263–269

Koga H, Fukahori S, Kitaoka T, Nakamura M, Wariishi H (2008a) Structured catalyst with porous fiber-network microstructure for autothermal hydrogen production. Chem Eng J 139:408–415

Koga H, Kitaoka T, Wariishi H (2008b) In situ synthesis of Cu nanocatalysts on ZnO whiskers embedded in a microstructured paper composite for autothermal hydrogen production. Chem Commun 43:5616–5618

Koga H, Umemura Y, Ishihara H, Kitaoka T, Tomoda A, Suzuki R, Wariishi H (2009) Structured fiber composites impregnated with platinum nanoparticles synthesized on a carbon fiber matrix for catalytic reduction of nitrogen oxides. Appl Catal B Environ 90:699–704

Liotta LF, Di Carlo G, Pantaleo G, Venezia AM, Deganello G (2006) $Co_3O_4/CeO_2$ composite oxides for methane emissions abatement: relationship between $Co_3O_4$–$CeO_2$ interaction and catalytic activity. Appl Catal B Environ 66:217–227

Liu S, Wu X, Weng D, Li M, Ran R (2015) Roles of acid sites on Pt/H-ZSM5 catalyst in catalytic oxidation of diesel soot. ACS Catal 5: 909–919

Luo JY, Meng M, Li X, Li XG, Zha YQ, Hu TD, Xie YN, Zhang J (2008) Mesoporous $Co_3O_4$–$CeO_2$ and Pd/$Co_3O_4$–$CeO_2$ catalysts: synthesis, characterization and mechanistic study of their catalytic properties for low-temperature CO oxidation. J Catal 254:310–324

Maksasithorn S, Praserthdam P, Suriye K, Debecker DP (2015) Preparation of super-microporous $WO_3$–$SiO_2$ olefin metathesis catalysts by the aerosol-assisted sol–gel process. Microporous Mesoporous Mater 213:125–133

Marrero-Jerez J, Larrondo S, Rodriguez-Castellón E, Núñez P (2014) TPR, XRD and XPS characterisation of ceria-based materials synthesized by freeze-drying precursor method. Ceram Int 40:6807–6814

Milt VG, Ulla MA, Miro EE (2005) NOx trapping and soot combustion on $BaCoO_{3-y}$ perovskite: LRS and FTIR characterization. Appl Catal B Environ 57:13–21

Mosconi S, Lick ID, Carrascull A, Ponzi MI, Ponzi EN (2007) Catalytic combustion of diesel soot: deactivation by $SO_2$ of copper and potassium nitrate catalysts supported on alumina. Catal Commun 8:1755–1758

Pega S, Boissiere C, Grosso D, Azais T, Chaumonnot A, Sanchez C (2009) Direct aerosol synthesis of large-pore amorphous mesostructured aluminosilicates with superior acid-catalytic properties. Angew Chem Int Ed 48:2784–2787

Piumetti M, Bensaid S, Russo N, Fino D (2016) Investigations into nanostructured ceria–zirconia catalysts for soot combustion. Appl Catal B Environ 180:271–282

Potoczna-Petru D, Kepinski L (2001) Reduction study of Co3O4 model catalyst by electron microscopy. Catal Lett 73:41–46

Quiles-Díaz S, Giménez-Mañogil J, García-García A (2015) Catalytic performance of $CuO/Ce_{0.8}Zr_{0.2}O_2$ loaded onto SiC-DPF in NOx-assisted combustion of diesel soot. RSC Adv 5(170):18–17029

Reichelt E, Heddrich MP, Jahn M, Michaelis A (2014) Fiber based structured materials for catalytic applications. Appl Catal A Gen 476:78–79

Santos GA, Santos CMB, da Silva SW, Urquieta-González EA, Confessori PP, Sartoratto (2012) Sol–gel synthesis of silica–cobalt composites by employing $Co_3O_4$ colloidal dispersions. Colloids Surf A Physicochem Eng Asp 395:217–224

Tarka A, Zyberta M, Kindler Z, Szmurlo J, Mierzwa B, Raróg-Pilecka W (2017) Effect of precipitating agent on the properties of cobalt catalysts promoted with cerium and barium for $NH_3$ synthesis obtained by co-precipitation. Appl Catal A Gen 532:19–25

Tuler FE, Banús ED, Zanuttini MA, Miró EE, Milt VG (2014) Ceramic papers as flexible structures for the development of novel diesel soot combustion catalysts. Chem Eng J 246:287–298

Tuler FE, Portela R, Ávila P, Banús ED, Miró EE, Milt VG (2015a) Structured catalysts based on sepiolite with tailored porosity to remove diesel soot. Appl Catal A Gen 498:41–53

Tuler FE, Gaigneaux EM, Miró EE, Milt VG, Debecker DP (2015b) Catalytic ceramic papers for diesel soot oxidation: a spray method for enhanced performance. Catal Commun 72:116–120

Xu W, Cai J, Zhou J, Ou Y, Long W, You Z, Lou Y (2016) Highly effective direct decomposition of nitric oxide by microwave catalysis over $BaMeO_3$ (Me= Mn, Co, Fe) mixed oxides at low temperature under excess oxygen. ChemCatChem 8:417–425

Yang X-L, Zhang W-Q, Xia C-G, Xiong X-M, Mu X-Y, Hu B (2010) Low temperature ruthenium catalyst for ammonia synthesis supported on $BaCeO_3$ nanocrystals. Catal Commun 11:867–870

Zhang H, Li S, Lin Q, Feng X, Chen Y, Wang J (2018) Study on hydrothermal deactivation of Pt/$MnO_x$-$CeO_2$ for $NO_x$-assisted soot oxidation: redox property, surface nitrates, and oxygen vacancies. Environ Sci Pollut Res 25:16061–16070. https://doi.org/10.1007/s11356-018-1582-5